

Adaptive Memory-Event-Triggered Static Output Control of T–S Fuzzy Wind Turbine Systems

Shen Yan , Zhou Gu , *Member, IEEE*, Ju H. Park , *Senior Member, IEEE*, and Xiangpeng Xie 

Abstract—This article studies the weighted memory-event-triggered H_∞ static output control issue of Takagi–Sugeno fuzzy wind turbine systems with uncertainty. To decrease the frequency of data communication, a novel adaptive memory-event-triggered mechanism is presented to choose the “necessary” control signals, which has the following two benefits. First, a weighted average signal over a historic period is utilized as the input of event-triggered scheme, instead of the current system information in the conventional one. This could reduce the control signal updating rate and avoid the false triggering events incurred by stochastic environment noises and disturbances. Second, a dynamic triggering threshold is adopted to adaptively regulate the control signal updating frequency along with the average signal. By applying the distributed delay system method to describe the weighted historic signal, a new uncertain T–S fuzzy wind turbine system with distributed delay is established. With the aid of the measured outputs and the integral inequality based on the weighting function of the average signal, the memory-event-triggered static output controller design conditions are obtained to ensure the system exponential stability and the H_∞ performance. Lastly, an experiment platform integrating Zigbee modules as the wireless network is set up to illustrate the advantages of the proposed strategy.

Index Terms—Distributed delay system, memory-event-triggered mechanism (ETM), static output control, Takagi–Sugeno (T–S) fuzzy system, wind turbine system (WTS).

I. INTRODUCTION

RECENTLY, due to the international consensus of the low-carbon economy, the development and utilization of

Manuscript received 1 August 2021; revised 16 November 2021; accepted 2 December 2021. Date of publication 9 December 2021; date of current version 1 September 2022. This work was supported in part by the National Natural Science Foundation of China under Grant 62103193 and Grant 62022044, in part by the Natural Science Foundation of Jiangsu Province of China under Grant BK20200769, in part by the Natural Science Foundation of Jiangsu Provincial Universities under Grant 20KJB510045, in part by Project funded by the China Postdoctoral Science Foundation under Grant 2021TQ0155, in part by the Jiangsu Natural Science Foundation for Distinguished Young Scholars under Grant BK20190039. The work of Ju H. Park was supported by the National Research Foundation of Korea (NRF), Korea Government (MSIT) under Grant 2020R1A2B5B02002002. (*Corresponding authors: Zhou Gu; Ju H. Park.*)

Shen Yan and Zhou Gu are with the College of Mechanical and Electronic Engineering, Nanjing Forestry University, Nanjing 210037, China (e-mail: yanshenzd@gmail.com; gzh1808@163.com).

Ju H. Park is with the Department of Electrical Engineering, Yeungnam University, Kyongsan 38541, Korea (e-mail: jessie@ynu.ac.kr).

Xiangpeng Xie is with the Institute of Advanced Technology, Nanjing University of Posts and Telecommunications, Nanjing 210023, China, and also with the School of Information Science and Engineering, Chengdu University, Chengdu 610106, China (e-mail: xiexiangpeng1953@163.com).

Color versions of one or more figures in this article are available at <https://doi.org/10.1109/TFUZZ.2021.3133892>.

Digital Object Identifier 10.1109/TFUZZ.2021.3133892

wind energy, a representative type of renewable clean energy, has attracted more and more attention and interest from global researchers [1]–[4]. Compared with traditional fossil energy and nuclear energy, wind energy is of higher efficiency and lower cost, which motivates the investigations for the stabilization problems of wind turbine systems (WTSs) [5]–[7]. Among various types of wind turbines, permanent magnetic synchronous generator (PMSG) is the widely used one owing to the merits, such as direct drive, slow rotation speed, and low maintenance cost.

However, the model of WTS with PMSG usually has nonlinearities, which is difficult to be handled in system stability analysis and control synthesis. As a powerful tool to deal with nonlinearities, Takagi–Sugeno (T–S) fuzzy method is effective to transform the nonlinear systems into a set of linear subsystems with appropriate membership functions. Regarding this topic, fruitful interesting outcomes about T–S fuzzy WTS have been derived (see [6], [8]–[10], and the references therein). Specifically, in [6], the sampled-data control issue for WTSs with actuator faults is addressed, where a series of linear subsystems is used to model the nonlinear dynamics of PMSG via the T–S fuzzy method. Hwang *et al.* [8] studied the disturbance observer-based sliding mode control problem for T–S fuzzy systems and its application to WTSs with a nonlinear PMSG. For a PMSG-based WTS, a T–S fractional-order fuzzy logic controller is designed in [9] to guarantee the system stability. It is noted that the abovementioned results are mostly dependent on the fact that all system states are measurable, which is a strong constraint for its application in real WTSs. To solve this problem, an observer is utilized in [10] to estimate the state, and the impulsive output controller is developed for T–S fuzzy PMSG-based WTSs. Different from the observer-based output control scheme, static output control is easier for executing in practical applications. In addition, it needs to be noted that since wind and moisture erosion, device aging, the system components will be unavoidably with uncertainties, which may lead to negative effect on control performance even deteriorate the system stability. Therefore, it is essential to investigate the static output control issue for uncertain T–S fuzzy WTSs.

On the other hand, as the popularization of communication technology and its applications in industry systems, networked control problem has become an interesting direction for WTSs, and some results can be found in [11]–[13]. For the abovementioned networked control strategies, the data are exchanged over the network channel with a time-triggered paradigm. Under such communication scheme, network congestion is highly possible

to occur when the system scale increases and many redundant packets are released. Thus, an effective communication scheme is required for WTSs to reduce the data transmission frequency and save the precious network resource. Over the past decade, the event-triggered mechanism (ETM) has been considered as an alternative manner to time-triggered paradigm [14]–[21]. Due to the aperiodic way to transmit the signal in some designed instants, the event-triggered control issues of WTSs have been investigated in [22] and [23]. For a fuzzy PMSG-based wind energy conversion systems with back to back converter, Prakash and Joo [22] designed an event-triggered controller for reducing the unnecessary communications and the data dropouts. The event-triggered reliable control problem for T–S fuzzy WTS with transmission delays is addressed in [23]. It is worth noting that the environment noises, abrupt disturbances, and uncertainties are inevitable for real systems. These phenomena may cause stochastic changes of system dynamics, and further lead to redundant and false triggers under the ETMs only with instantaneous system information in [22]. Mousavi and Marquez [24] provided an integral-based ETM with the average signal over a time interval to suppress the effect of measurement noises. In [25], an integral-event-triggered scheme utilizing the historic system states is presented to develop an event-triggered H_∞ controller for T–S fuzzy systems. The same weight is used to match the past information of ETMs in [24] and [25], while it is more practical and logical to choose a variable weighting function for different states. Moreover, the amount of event-triggers is affected by the triggering thresholds. Most of them in the above-mentioned ETMs are constant and cannot be adjusted dynamically to the system dynamics. For T–S fuzzy uncertain WTSs, fewer studies have been conducted for the adaptive memory-event-triggered H_∞ static output control problem with a variable weighting function and a dynamic triggering threshold.

In light of the aforementioned observations, the contributions of this article are as follows.

- 1) The historic system outputs with a variable weighting function is used to design a novel adaptive weighted METM, where a sleep period is introduced to exclude accumulation triggers. Compared with the normal switching ETM [15], the weighted METM is beneficial to reduce more redundant and false triggers induced by high-frequency noises and disturbances. Meanwhile, an adaptive law related with the weighted historic system outputs is constructed to adapt the triggering threshold dynamically.
- 2) The weighted memory-event-triggered static output control WTS with nonlinearity and uncertainty under is modeled by a new switched T–S fuzzy uncertain system. One subsystem is denoted by an interval time-varying delay system over the sleep interval. The other subsystem is described via a T–S fuzzy uncertain distributed delay system, in which the weighting function is treated as the distributed delay kernel.
- 3) Different from the integral inequality related with Legendre polynomials to approximate the distributed delay with kernel in [29], applying the integral inequality using the kernel directly can avoid approximation error, and

obtain less conservative event-triggered H_∞ static output controller design conditions for PMSG-based WTSs. Moreover, a real wireless network with ZigBee modules is built up to transmit control signals and the effectiveness of the proposed approach is tested on this experimental setup.

The rest of this article is structured as follows. Section II presents the preliminaries of the investigated issue. In Section III, the stability and synthesis criteria of the considered WTSs are derived. In Section IV, the simulation results are executed. Finally, Section V concludes this article.

Notation: In this article, Y^T means the transpose of a matrix or vector Y , $\flat(X, Y)$ and $\sharp(X)$ stand for $Y^T X Y$ and $X^T + X$, respectively, and \otimes means Kronecker product.

II. PRELIMINARIES

This section gives a WTS with a nonlinear PMSG modeled by a T–S fuzzy system. A brief framework of the PMSG-based WTS is shown in Fig. 1.

A. Wind Turbine Aerodynamic Torque

According to aerodynamics, the power extracted from the wind is represented as

$$\mathbb{P}_t = \frac{1}{2} \vartheta \pi \mathbb{R}^2 \mathbb{C}_p(\alpha(t), \beta) v_w^3(t) \quad (1)$$

where ϑ , \mathbb{R} , and $v_w(t)$ represent the air density, blade length, wind speed, respectively, the power coefficient is denoted by $\mathbb{C}_p(\alpha(t), \beta)$, in which $\alpha(t) = v_t(t)\mathbb{R}/v_w(t)$ means the tip speed ratio, β is the pitch angle, and $v_t(t)$ stands for the turbine rotational speed. Based on [26], we have

$$\mathbb{C}_p(\alpha(t), \beta) = 0.22 \left(\frac{116}{\alpha_i(t)} - 0.4\beta - 5 \right) e^{-\frac{12.5}{\alpha_i(t)}}$$

where

$$\frac{1}{\alpha_i(t)} = \frac{1}{\alpha(t) + 0.08\beta} - \frac{0.035}{\beta^3 + 1}.$$

To derive the optimal energy, the optimum value of $\mathbb{C}_{p \max}(\alpha(t), \beta)$ is considered for wind turbine by taking $\alpha(t) = \alpha_{\text{opt}}(t)$. The aerodynamic torque is obtained as

$$\mathbb{T}_m(t) = \frac{\mathbb{P}_t}{v_t} = \frac{\mathbb{C}_p(\alpha(t), \beta) \vartheta \pi \mathbb{R}^3 v_w^2(t)}{2\alpha(t)}. \quad (2)$$

B. T–S Fuzzy Model of PMSG-Based WTS

In terms of [27], the dynamics of PMSG with uncertainty and wind turbine are described as follows:

$$\begin{cases} \dot{\mathbb{V}}_d(t) = (\mathbb{R}_s + \Delta R) i_d(t) + \mathbb{L}_d \frac{di_d(t)}{dt} \\ \quad - w_e(t) \mathbb{L}_q i_q(t) + f_1 \mathbb{U}_f(t) \\ \dot{\mathbb{V}}_q(t) = (\mathbb{R}_s + \Delta R) i_q(t) + \mathbb{L}_q \frac{di_q(t)}{dt} \\ \quad + w_e(t) \mathbb{Q}_f + f_2 \mathbb{U}_f(t) \\ \dot{w}_g(t) = \frac{1}{\mathbb{J}} (\mathbb{T}_e(t) - \mathbb{T}_m(t) - \rho w_g(t)) + f_3 \mathbb{U}_f(t) \\ \mathbb{T}_e(t) = \frac{3}{2} \mathbb{P}_n i_q(t) \mathbb{Q}_f \end{cases} \quad (3)$$

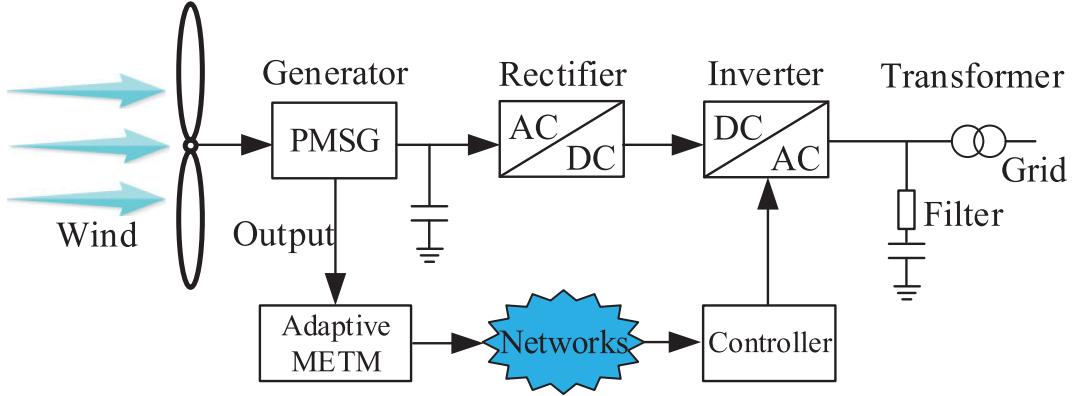


Fig. 1. Structure of PMSG-based WTS with an adaptive METM.

where \mathbb{P}_n means the number of poles, $w_g(t)$ represents the rotor speed, \mathbb{R}_s and ΔR are the stator resistance and its uncertainty, respectively, \mathbb{L}_d and \mathbb{L}_q stand for the stator inductance on the d - q axis, \mathbb{Q}_f means the magnetic flux of the permanent magnet, $\mathbb{T}_e(t)$ is the generator torque, $w_e(t) = \mathbb{P}_n w_g(t)$, $\mathbb{U}_f(t)$ is the external disturbance, and \mathbb{J} and ρ are the moment of inertia and the friction coefficient, respectively.

Then, by selecting $x(t) = [x_1(t) \ x_2(t) \ x_3(t)]^\top = [w_g(t) \ i_q(t) \ i_d(t)]^\top$, $g(t) = [w_g(t) \ i_q(t)]^\top$, and $\varpi(t) = \mathbb{U}_f(t)$ as the state, output, and external disturbance, respectively, the state-space model of WTS can be established as

$$\begin{cases} \dot{x}(t) = (\mathfrak{A} + \Delta\mathfrak{A})x(t) + \mathfrak{B}u(t) + \mathfrak{F}\varpi(t) \\ g(t) = \mathfrak{C}x(t) \\ z(t) = \mathfrak{H}x(t) \end{cases} \quad (4)$$

where $z(t)$ denotes the controlled output, the controller is represented by $u(t) = [\mathbb{V}_q(t) \ \mathbb{V}_d(t)]^\top$. Then, the system matrices are formulated as

$$\mathfrak{A} = \begin{bmatrix} \frac{-\rho + \mathbb{T}_0 w_g(t)}{\mathbb{J}} & \frac{3\mathbb{P}_n \mathbb{Q}_f}{2\mathbb{J}} & 0 \\ -\frac{\mathbb{P}_n \mathbb{Q}_f}{\mathbb{L}_q} & -\frac{\mathbb{L}_q}{\mathbb{R}_s} & -\frac{\mathbb{P}_n w_g(t) \mathbb{L}_d}{\mathbb{L}_q} \\ 0 & \frac{\mathbb{P}_n w_g(t) \mathbb{L}_q}{\mathbb{L}_d} & -\frac{\mathbb{R}_s}{\mathbb{L}_d} \end{bmatrix}$$

$$\Delta\mathfrak{A} = \mathfrak{D}_1 \Delta\hat{R} \mathfrak{D}_2, \quad \Delta\hat{R} = \begin{bmatrix} \frac{\Delta R}{d} & 0 \\ 0 & \frac{\Delta R}{d} \end{bmatrix}, \quad \mathfrak{D}_2 = \begin{bmatrix} 0 & d & 0 \\ 0 & 0 & d \end{bmatrix}$$

$$\mathfrak{D}_1 = \begin{bmatrix} 0 & 0 \\ -\frac{1}{\mathbb{L}_q} & 0 \\ 0 & -\frac{1}{\mathbb{L}_d} \end{bmatrix}, \quad \mathfrak{B} = \begin{bmatrix} 0 & 0 \\ \frac{1}{\mathbb{L}_q} & 0 \\ 0 & \frac{1}{\mathbb{L}_d} \end{bmatrix}, \quad \mathfrak{F} = \begin{bmatrix} f_1 \\ f_2 \\ f_3 \end{bmatrix}$$

$$\mathfrak{C} = \mathfrak{H} = \begin{bmatrix} 1 & 0 & 0 \\ 0 & 1 & 0 \end{bmatrix}, \quad \mathbb{T}_0 = \frac{C_{p\max} \vartheta \pi \mathbb{R}^5}{2\alpha_{\text{opt}}^3(t)}$$

where d is the upper bound of the uncertainty ΔR ($|\Delta R| \leq d$). $\Delta\mathfrak{A}$ is assumed to satisfy the following norm-bound condition [31]:

$$\Delta\mathfrak{A} + \Delta\mathfrak{A}^\top \leq \nu \mathfrak{D}_1^\top \mathfrak{D}_1 + \nu^{-1} \mathfrak{D}_2^\top \mathfrak{D}_2 \quad (5)$$

where $\nu > 0$ and $\Delta\hat{R}^\top \Delta\hat{R} \leq I$.

In order to obtain the stability condition of nonlinear system (4), the T-S fuzzy method is used to describe it as follows.

Plant Rule i: IF $w_g(t)$ is ψ_i , THEN

$$\begin{cases} \dot{x}(t) = (\mathfrak{A}_i + \Delta\mathfrak{A})x(t) + \mathfrak{B}u(t) + \mathfrak{F}\varpi(t) \\ g(t) = \mathfrak{C}x(t) \\ z(t) = \mathfrak{H}x(t) \end{cases} \quad (6)$$

where $w_g(t) = x_1(t) \in [x_{1\min} \ x_{1\max}] = [\mathbb{D}_1 \ \mathbb{D}_2]$ is the premise variable, ψ_i^s ($s = 1, \dots, p$) means the fuzzy set for i th rule ($i = 1, \dots, q$), $p = 1$ and $q = 2$ are the number of premise variables and fuzzy rules, respectively, and

$$\mathfrak{A}_1 = \begin{bmatrix} \frac{-\rho + \mathbb{T}_0 \mathbb{D}_1}{\mathbb{J}} & \frac{2\mathbb{P}_n \mathbb{Q}_f}{2\mathbb{J}} & 0 \\ -\frac{\mathbb{P}_n \mathbb{Q}_f}{\mathbb{L}_q} & -\frac{\mathbb{L}_q}{\mathbb{R}_s} & -\frac{\mathbb{P}_n \mathbb{D}_1 \mathbb{L}_d}{\mathbb{L}_q} \\ 0 & \frac{\mathbb{P}_n \mathbb{D}_1 \mathbb{L}_q}{\mathbb{L}_d} & -\frac{\mathbb{R}_s}{\mathbb{L}_d} \end{bmatrix}$$

$$\mathfrak{A}_2 = \begin{bmatrix} \frac{-\rho + \mathbb{T}_0 \mathbb{D}_2}{\mathbb{J}} & \frac{2\mathbb{P}_n \mathbb{Q}_f}{2\mathbb{J}} & 0 \\ -\frac{\mathbb{P}_n \mathbb{Q}_f}{\mathbb{L}_q} & -\frac{\mathbb{L}_q}{\mathbb{R}_s} & -\frac{\mathbb{P}_n \mathbb{D}_2 \mathbb{L}_d}{\mathbb{L}_q} \\ 0 & \frac{\mathbb{P}_n \mathbb{D}_2 \mathbb{L}_q}{\mathbb{L}_d} & -\frac{\mathbb{R}_s}{\mathbb{L}_d} \end{bmatrix}.$$

Then, the uncertain T-S fuzzy WTS with PMSG is represented by

$$\begin{cases} \dot{x}(t) = \sum_{i=1}^2 \theta_i(t) ((\mathfrak{A}_i + \Delta\mathfrak{A})x(t) + \mathfrak{B}u(t) + \mathfrak{F}\varpi(t)) \\ g(t) = \mathfrak{C}x(t) \\ z(t) = \mathfrak{H}x(t) \end{cases} \quad (7)$$

where $\theta_i(t)$ denotes the normalized membership function, and satisfies

$$\theta_1(t) = \frac{\mathbb{D}_2 - x_1(t)}{\mathbb{D}_2 - \mathbb{D}_1}, \quad \theta_2(t) = 1 - \theta_1(t)$$

$$\sum_{i=1}^2 \theta_i(t) = 1, \quad x_1(t) = \theta_1(t)\mathbb{D}_1 + \theta_2(t)\mathbb{D}_2.$$

Remark 1: Since temperature changes, device aging, the values of system components could be with uncertainties. In (3), the uncertainty of stator resistance is considered in the system modeling. Thus, a more general uncertain T-S fuzzy WTS is established than the existing models in [5], [6], [22], and [23].

C. Adaptive Weighted METM

To release the network transmission burden, an adaptive METM with a variable weighting function is constructed to determine a new triggering time of control signal, which is given as

$$t_{k+1} = \min_t \{t \geq t_k + \eta | \phi(t) \geq 0\} \quad (8)$$

where $\phi(t) = e^\top(t)\Omega e(t) - \sigma(t)g^{*\top}(t)\Omega g^*(t)$, $g^*(t) \triangleq \int_{-\lambda}^0 w(s)g(t+s)ds$, $e(t) = g^*(t) - g(t_k) = \int_{-\lambda}^0 w(s)g(t+s)ds - g(t_k)$, t_k and t_{k+1} are the latest and next triggering times, respectively, $\Omega > 0$, $\eta > 0$ is the sleep interval, and $\lambda > 0$ denotes the period of past outputs. $\sigma(t) \in [\sigma_m, \sigma_M]$ ($0 < \sigma_m \leq \sigma_M < 1$) is an adaptive triggering threshold governed by the regulating rule

$$\sigma(t) = \sigma_m \left(1 - e^{-\|g^*(t)\|}\right) + \sigma_M e^{-\|g^*(t)\|}. \quad (9)$$

The weighting function, $w(s)$, is utilized to describe the weights of historic outputs at different times, and is supposed to meet $\int_{-\lambda}^0 w(s)ds = 1$.

Remark 2: From the definition of $g^*(t)$ in (8), it is observed that the output error $e(t)$ is different from the error $g(t) - g(t_k)$ in some conventional ETMs. In (8), the weighted mean of historic outputs over time interval $[t - \lambda, t]$, $g^*(t)$, is utilized to replace $g(t)$. With this treatment, the presented METM is useful for decrease the redundant and false triggers induced by disturbances or noises with high frequency. In addition, the weighting function $w(s)$ is usually chosen as an increasing function over $s \in [t - \lambda, t]$. For instance, in the simulation section, $w(s) = \frac{\pi}{2\eta} \cos(\frac{\pi}{2\eta}s)$ for $s \in [t - \lambda, t]$ is considered as the weighting function, which implies that the weight of the output $g(t + s)$ increases from the past time $t - \lambda$ to the current time t .

Remark 3: The adaptive triggering threshold $\sigma(t)$ in (8) is dependent on the weighted mean of historic outputs $g^*(t)$. To be specific, $\sigma(t)$ increases as the decrease of the value of $\|g^*(t)\|$. The motivation of the adaptive law is that more signals should be released to improve the control performance when $g^*(t)$ deviates from the steady state, while fewer signals is required if $g^*(t)$ is close to the equilibrium point. Compared with the existing ETMs with constant thresholds, the adaptive METM (8) is able to adjust the number of triggering events dynamically according

to the requirement of system performance, which means it is more applicable for practical systems.

Remark 4: When $\sigma_m = \sigma_M$ and $\lambda \rightarrow 0$, the proposed METM (8) reduces to the switching ETM in [15]. In addition, if $\sigma_m = \sigma_M$, $w(s) = \frac{1}{\lambda}$, and $\eta = 0$, METM (8) equals to the integral-based ETM in [25]. These indicate that the proposed METM covers some existing ETMs as special cases. Moreover, a positive time period η is added after each triggering event in the METM, which is the lower bound of interevent interval. Thus, Zeno behavior is avoided.

By considering the triggering condition (8), the robust T-S fuzzy event-triggered controller is formed as

$$u(t) = \sum_{j=1}^q \vartheta_j(t_k) \mathfrak{K}_j g(t_k)$$

$$= \begin{cases} \sum_{j=1}^q \vartheta_j^k \mathfrak{K}_j \mathfrak{C} x(t - \eta(t)), & t \in \mathcal{T}_1 \\ \sum_{j=1}^q \vartheta_j^k \mathfrak{K}_j \left(\mathfrak{C} \int_{-\lambda}^0 w(s)x(t+s)ds - e(t) \right), & t \in \mathcal{T}_2 \end{cases} \quad (10)$$

where $\eta(t) \triangleq t - t_k \in [0, \eta]$ for $t \in \mathcal{T}_1 \triangleq [t_k, t_k + \eta)$, $\mathcal{T}_2 \triangleq [t_k + \eta, t_{k+1})$, and $\mathcal{T} \triangleq \mathcal{T}_1 \cup \mathcal{T}_2$.

For the simplification of expression, $\theta_i(t)$ and $\vartheta_j(t_k)$ are written as θ_i and ϑ_j^k in the following part, respectively. In addition, the same assumption $\vartheta_j^k - \rho_j \theta_j \geq 0$ with [8] is introduced.

Defining

$$\mathbb{W}_x(t) = \int_{-\lambda}^0 W(s)x(t+s)ds, \quad W(s) = \mathbf{w}(s) \otimes I_3$$

$$\mathbf{w}(s) = [w_0(s); w_1(s); \dots; w_\kappa(s)], \quad w(s) = w_0(s)$$

$$\mathcal{I} = [I_3 \ 0_{3,3\kappa}] \quad (11)$$

one obtains

$$\int_{-\lambda}^0 w(s)x(t+s)ds = \mathcal{I} \mathbb{W}_x(t) \quad (12)$$

where $w_i(s)$ is independent element, $\mathbf{w}(s)$ satisfies $\dot{\mathbf{w}}(s) = \mathcal{W}\mathbf{w}(s)$, and \mathcal{W} is the coefficient matrix.

By combing (10), (12), and (4), the event-triggered WTS is obtained as

$$\dot{x}(t) = \sum_{i=1}^2 \sum_{j=1}^2 \theta_i \vartheta_j^k [(\mathfrak{A}_i + \Delta \mathfrak{A})x(t) + \mathfrak{B}_{lj} + \mathfrak{F}\varpi(t)], \quad t \in \mathcal{T} \quad (13)$$

where

$$\mathfrak{B}_{lj} = \begin{cases} \mathfrak{B} \mathfrak{K}_j \mathfrak{C} x(t - \eta(t)), & t \in \mathcal{T}_1, l = 1 \\ \mathfrak{B} \mathfrak{K}_j (\mathfrak{C} \mathcal{I} \mathbb{W}_x(t) - e(t)), & t \in \mathcal{T}_2, l = 2 \end{cases}$$

This work aims to solve the controller gains in (10) such that the following hold.

- 1) The uncertain T-S fuzzy WTS (13) is exponentially stable for $\varpi(t) \equiv 0$.
- 2) The H_∞ level $\int_0^\infty z^\top(t)z(t)dt < \gamma^2 \int_0^\infty \varpi^\top(t)\varpi(t)dt$ is guaranteed with a scalar $\gamma > 0$ for $\varpi(t) \neq 0$ and $x(0) = 0$.

Before further proceeding, we produce the following lemma.

Lemma 1: [28] For the vector $w(s)$ defined in (11) and the matrix $\mathfrak{R} > 0$, one can get

$$\int_{-\lambda}^0 x^\top(s) \mathfrak{R} x(s) ds \geq b(\Psi \otimes \mathfrak{R}, \mathbb{W}_x(t)) \quad (14)$$

where $\Psi^{-1} = \int_{-\lambda}^0 w(s) w^\top(s) ds$.

III. MAIN RESULTS

In this section, the criterions are first established in Theorem 1 for guaranteeing the H_∞ stability of system (13). Then, we will design the controller gains in (10) and the triggering matrix in (8) based on the criterions in Theorem 2.

For facilitating the derivations of the main results, we define

$$\mathcal{J}_a^1 \triangleq \begin{cases} \begin{bmatrix} 0_{3,3(a-1)} & I_3 & 0_{3,8(6+\kappa-a)+3} \end{bmatrix}, & a = 1, \dots, 6 + \kappa \\ \begin{bmatrix} 0_{1,3(6+\kappa)} & 1 & 0_{1,2} \end{bmatrix}, & a = 7 + \kappa \\ \begin{bmatrix} 0_{2,3(6+\kappa)+1} & I_2 \end{bmatrix}, & a = 8 + \kappa \end{cases}$$

$$\mathcal{J}_a^2 \triangleq \begin{cases} \begin{bmatrix} 0_{3,3(a-1)} & I_3 & 0_{3,3(5+\kappa-a)+5} \end{bmatrix}, & a = 1, \dots, 5 + \kappa \\ \begin{bmatrix} 0_{2,3(5+\kappa)} & I_2 & 0_{2,3} \end{bmatrix}, & a = 6 + \kappa \\ \begin{bmatrix} 0_{1,3(5+\kappa)+2} & 1 & 0_{1,2} \end{bmatrix}, & a = 7 + \kappa \\ \begin{bmatrix} 0_{2,3(5+\kappa)+3} & I_2 \end{bmatrix}, & a = 8 + \kappa \end{cases}.$$

Theorem 1: For given positive scalars $\rho_j, \sigma_M, \eta, \lambda, \mu$, and ν , the uncertain T-S fuzzy system (13) under the adaptive weighted METM (8) is exponentially stable, satisfying the decay rate ς and H_∞ level γ , if there exist symmetric matrices $\mathfrak{R}_1, \mathfrak{R}_i > 0$ ($i = 2, 3, 4, 5$), $\mathfrak{R}_5 > 0$, and matrices $\Lambda_{li}, \mathfrak{R}_j$, and X such that

$$\bar{\mathfrak{R}}_1 > 0 \quad (15)$$

$$\rho_j(\Xi_{lij} + \#(\mathfrak{X}_l \Delta \mathfrak{A} \mathcal{J}_2^l) - \Lambda_{li}) < 0 \quad (16)$$

$$\rho_i(\Xi_{lii} + \#(\mathfrak{X}_l \Delta \mathfrak{A} \mathcal{J}_2^l) - \Lambda_{li}) + \Lambda_{li} < 0 \quad (17)$$

$$\rho_j(\Xi_{lij} + \#(\mathfrak{X}_l \Delta \mathfrak{A} \mathcal{J}_2^l) - \Lambda_{li}) + \Lambda_{li}$$

$$+ \rho_i(\Xi_{lji} + \#(\mathfrak{X}_l \Delta \mathfrak{A} \mathcal{J}_2^l) - \Lambda_{lj}) + \Lambda_{lj} < 0 \quad (i < j) \quad (18)$$

for $l = 1, 2$, where

$$e^{-2\varsigma\lambda} \triangleq \lambda_e, \quad e^{-2\varsigma\eta} \triangleq \eta_e$$

$$\bar{\mathfrak{R}}_1 = \mathfrak{R}_1 + \text{diag}\{0, \lambda_e(\Psi \otimes \mathfrak{R}_3)\}, \quad \widehat{W} = W \otimes I_3$$

$$\Xi_{1ij} = \Pi_1 + \#(\mathfrak{X}_1 \mathfrak{G}_{1ij}), \quad \mathfrak{X}_1 = (X \mathcal{J}_1^1 + \mu X \mathcal{J}_2^1)^\top$$

$$\begin{aligned} \Pi_1 &= \#(\mathfrak{M}_1^\top \mathfrak{R}_1 \mathfrak{M}_1) + 2\varsigma b(\mathfrak{R}_1, \mathfrak{M}_1) \\ &+ \#(\mathcal{J}_{8+\kappa}^{1\top} \mathfrak{C} \mathcal{J}_2^1) - \frac{\eta_e}{\eta} b(\bar{\mathfrak{R}}_5, \mathbb{I}_1) + F^1 \end{aligned}$$

$$\mathfrak{G}_{1ij} = \mathfrak{A}_i \mathcal{J}_2^1 + \mathfrak{B} \mathfrak{R}_j \mathfrak{C} \mathcal{J}_{6+\kappa}^1 + \mathfrak{F} \mathcal{J}_{7+\kappa}^1 - I \mathcal{J}_1^1$$

$$\mathfrak{M}_1 = \begin{bmatrix} \mathcal{J}_2^1 \\ \hat{\mathcal{J}}_\lambda^1 \end{bmatrix}, \quad \mathfrak{N}_1 = \begin{bmatrix} \mathcal{J}_1^1 \\ W(0) \mathcal{E}_2^1 - W(-\lambda) \mathcal{J}_4^1 - \widehat{W} \hat{\mathcal{J}}_\lambda^1 \end{bmatrix}$$

$$\hat{\mathcal{J}}_\lambda^1 = \begin{bmatrix} \mathcal{J}_5^1 \\ \vdots \\ \mathcal{J}_{5+\kappa}^1 \end{bmatrix}, \quad \mathbb{I}_1 = \begin{bmatrix} \mathcal{J}_2^1 - \mathcal{J}_6^1 \\ \mathcal{J}_6^1 - \mathcal{J}_3^1 \end{bmatrix}, \quad \bar{\mathfrak{R}}_5 = \begin{bmatrix} \mathfrak{R}_5 & U \\ U^\top & \mathfrak{R}_5 \end{bmatrix}$$

$$F^1 = \text{diag}\{F_1^1, F_2^1, F_3^1, F_4^1, F_5^1, 0, -\gamma^2 I, -I\}$$

$$F_1^1 = \eta \mathfrak{R}_5, \quad F_2^1 = \mathfrak{R}_2 + \mathfrak{R}_3 + \lambda \mathfrak{R}_4$$

$$F_3^1 = -\eta_e \mathfrak{R}_2, \quad F_4^1 = -\lambda_e \mathfrak{R}_3, \quad F_5^1 = -\lambda_e(\Psi \otimes \mathfrak{R}_4)$$

$$\Xi_{2ij} = \Pi_2 + \#(\mathfrak{X}_2 \mathfrak{G}_{2ij})$$

$$\begin{aligned} \Pi_2 &= \#(\mathfrak{M}_2^\top \mathfrak{R}_1 \mathfrak{M}_2) + 2\varsigma \mathfrak{M}_2^\top \mathfrak{R}_1 \mathfrak{M}_2 \\ &+ \#(\mathcal{J}_{8+\kappa}^{2\top} \mathfrak{C} \mathcal{J}_2^2) - \frac{\eta_e}{\eta} b(\mathfrak{R}_5, \mathbb{I}_2) + F^2 \end{aligned}$$

$$\mathfrak{X}_2 = (X \mathcal{J}_1^2 + \mu X \mathcal{J}_2^2)^\top, \quad \mathbb{I}_2 = \begin{bmatrix} \mathcal{J}_2^2 - \mathcal{J}_3^2 \end{bmatrix}$$

$$\mathfrak{G}_{2ij} = (\mathfrak{A}_i + \Delta \mathfrak{A}) \mathcal{J}_2^2 + \mathfrak{B} \mathfrak{R}_j \mathfrak{C} \mathcal{J}_5^2 - \mathfrak{B} \mathfrak{R}_j \mathcal{J}_{6+\kappa}^2 + \mathfrak{F} \mathcal{J}_{7+\kappa}^2 - I \mathcal{J}_1^2$$

$$\mathfrak{M}_2 = \begin{bmatrix} \mathcal{J}_2^2 \\ \hat{\mathcal{J}}_\lambda^2 \end{bmatrix}, \quad \mathfrak{N}_2 = \begin{bmatrix} \mathcal{J}_1^2 \\ W(0) \mathcal{J}_2^2 - W(-\lambda) \mathcal{J}_4^2 - \widehat{W} \hat{\mathcal{J}}_\lambda^2 \end{bmatrix}$$

$$\hat{\mathcal{J}}_\lambda^2 = \begin{bmatrix} \mathcal{J}_5^{2\top} & \dots & \mathcal{J}_{5+\kappa}^{2\top} \end{bmatrix}^\top$$

$$F^2 = \text{diag}\{F_1^2, F_2^2, F_3^2, F_4^2, F_5^2, -\Omega, -\gamma^2 I, -I\}$$

$$F_1^2 = F_1^1, \quad F_2^2 = F_2^1, \quad F_3^2 = F_3^1, \quad F_4^2 = F_4^1$$

$$F_5^2 = -\lambda_e(\Psi \otimes \mathfrak{R}_4) + \sigma_M b(\Omega, \mathfrak{C} \mathcal{J}).$$

Proof: We define $\xi(t) = \begin{bmatrix} x(t) \\ \mathbb{W}_x(t) \end{bmatrix}$, and choose the following Lyapunov–Krasovskii functional (LKF):

$$\begin{aligned} V(t) &= \xi^\top(t) \mathfrak{R}_1 \xi(t) + \int_{t-\eta}^t e^{2\varsigma(s-t)} x^\top(s) \mathfrak{R}_2 x(s) ds \\ &+ \int_{t-\lambda}^t e^{2\varsigma(s-t)} x^\top(s) [\mathfrak{R}_3 + (s-t+\lambda) \mathfrak{R}_4] x(s) ds \\ &+ \int_{-\eta}^0 \int_{t+v}^t e^{2\varsigma(s-t)} \dot{x}^\top(s) \mathfrak{R}_5 \dot{x}(s) ds dv. \end{aligned} \quad (19)$$

Adopting Lemma 1 to cope with $\int_{t-\lambda}^t e^{2\varsigma(s-t)} b(\mathfrak{R}_3, x(s)) ds$, gives

$$\int_{t-\lambda}^t e^{2\varsigma(s-t)} b(\mathfrak{R}_3, x(s)) ds \geq \lambda_e b(\Psi \otimes \mathfrak{R}_3, \mathbb{W}_x(t)). \quad (20)$$

According to (19) and (20), it yields

$$\begin{aligned} V(t) &\geq b(\mathfrak{R}_1, \xi(t)) + \int_{-\eta}^0 e^{2\varsigma s} b(\mathfrak{R}_2, x(t+s)) ds \\ &+ \lambda_e b(\Psi \otimes \mathfrak{R}_3, \mathbb{W}_x(t)) + \int_{-\lambda}^0 e^{2\varsigma s} b((s+\lambda) \mathfrak{R}_4, x(t+s)) ds \\ &+ \int_{-\eta}^0 \int_{t+v}^t e^{2\varsigma s} \dot{x}^\top(s) \mathfrak{R}_5 \dot{x}(s) ds dv. \end{aligned} \quad (21)$$

Therefore, $V(t) > 0$ is guaranteed by $\mathfrak{R}_2 > 0, \mathfrak{R}_4 > 0, \bar{\mathfrak{R}}_1 > 0$.

Then, we calculate $\dot{V}(t)$ as

$$\dot{V}(t) + 2\varsigma V(t) \triangleq \mathcal{V}(t) \quad (22)$$

where

$$\begin{aligned} \mathcal{V}(t) = & \xi^\top(t) \mathfrak{R}_1 \dot{\xi}(t) + 2\varsigma b(\mathfrak{R}_1, \xi(t)) \\ & + b(\mathfrak{R}_2 + \mathfrak{R}_3 + \lambda \mathfrak{R}_4, x(t)) - b(\eta_e \mathfrak{R}_2, x(t - \eta)) \\ & - \lambda_e b(\mathfrak{R}_3, x(t - \lambda)) - \lambda_e \int_{-\lambda}^0 b(\mathfrak{R}_4, x(t + s)) ds \\ & + \eta b(\mathfrak{R}_5, \dot{x}(t)) - \eta_e \int_{-\eta}^0 b(\mathfrak{R}_5, x(t + s)) ds. \end{aligned}$$

The system (13) is guaranteed to be H_∞ exponentially stable once the following inequality holds:

$$\mathcal{J}(t) \triangleq \mathcal{V}(t) + z^\top(t) z(t) - \gamma^2 \varpi^\top(t) \varpi(t) < 0. \quad (23)$$

The integral term $-\lambda_e \int_{-\lambda}^0 b(\mathfrak{R}_4, x(t + s)) ds$ in (23) can be relaxed via Lemma 1 as

$$-\lambda_e \int_{-\lambda}^0 b(\mathfrak{R}_4, x(t + s)) ds \leq -\lambda_e b(\Psi \otimes \mathfrak{R}_4, \mathbb{W}_x(t)). \quad (24)$$

Next, two cases are taken into consideration.

Case I ($t \in \mathcal{T}_1$): The system (13) is formulated as

$$\dot{x}(t) = \sum_{j=1}^q \theta_j \vartheta_j^k [(\mathfrak{A}_i + \Delta \mathfrak{A})x(t) + \mathfrak{B} \mathfrak{K}_j \mathfrak{C} x(t - \eta(t)) + \mathfrak{F} \varpi(t)]. \quad (25)$$

Therefore, we can express the system (25) as

$$\sum_{i=1}^q \sum_{j=1}^q \theta_i \vartheta_j^k \mathfrak{G}_{1ij} \chi_1(t) = 0 \quad (26)$$

where $\chi_1^\top(t) \triangleq [\hat{x}^\top(t) \ x^\top(t) \ x^\top(t - \eta) \ x^\top(t - \lambda) \ \mathbb{W}_x^\top(t) \ x^\top(t - \eta(t)) \ \varpi^\top(t) \ z^\top(t)]$.

According to the property $\dot{w}(s) = \mathcal{W}w(s)$, it yields

$$\dot{\mathbb{W}}_x(t) = W(0)x(t) - W(-\lambda)x(t - \lambda) - \widehat{\mathcal{W}} \mathbb{W}_x(t). \quad (27)$$

Then, one can denote $\xi(t)$ and $\dot{\xi}(t)$ by

$$\xi(t) = \mathfrak{M}_1 \chi_1(t), \quad \dot{\xi}(t) = \mathfrak{N}_1 \chi_1(t). \quad (28)$$

From $\bar{\mathfrak{R}}_5 > 0$ and adopting the reciprocally convex lemma [30] to treat $-\eta_e \int_{-\eta}^0 b(\mathfrak{R}_5, x(t + s)) ds$, it leads to

$$-\eta_e \int_{-\eta}^0 b(\mathfrak{R}_5, x(t + s)) ds \leq -\frac{\eta_e}{\eta} b(\mathbb{I}_1^\top \bar{\mathfrak{R}}_5 \mathbb{I}_1, \chi_1(t)). \quad (29)$$

By combing (23), (24), (28), and (29), one can derive

$$\chi_1^\top(t) \mathbb{I}_1 \chi_1(t) < 0. \quad (30)$$

Based on (25) and choosing $\mathfrak{X}_1 = X \mathcal{J}_1^1 + \mu X \mathcal{J}_1^2$, we have

$$\sum_{i=1}^q \sum_{j=1}^q \theta_i \vartheta_j^k \chi_1^\top(t) \#(\mathfrak{X}_1 \mathfrak{G}_{1ij}) \chi_1(t) < 0. \quad (31)$$

Computing the sum of (30) and (31), yields

$$\sum_{i=1}^q \sum_{j=1}^q \theta_i \vartheta_j^k \chi_1^\top(t) (\Xi_{lij} + \#(\mathfrak{X}_1^\top \Delta \mathfrak{A} \mathcal{J}_2^1)) \chi_1(t) < 0 \quad (32)$$

where $\Xi_{lij} = \mathbb{I}_1 + \#(\mathfrak{X}_1 \mathfrak{G}_{1ij})$.

Employing the assumption $\vartheta_j^k - \rho_j \theta_j > 0$ in [8] to deal with the problem of membership function mismatch, one obtains

$$\begin{aligned} & \sum_{i=1}^q \sum_{j=1}^q \theta_i \vartheta_j^k \chi_1^\top(t) (\Xi_{lij} + \#(\mathfrak{X}_1 \Delta \mathfrak{A} \mathcal{J}_2^1)) \chi_1(t) \\ & \leq \sum_{i=1}^q \sum_{j=1}^q \theta_i \theta_j \chi_1^\top(t) [\rho_i (\Xi_{1ii} + \#(\mathfrak{X}_1 \Delta \mathfrak{A} \mathcal{J}_2^1 - \Lambda_{1i}) + \Lambda_{1i}) \chi_1(t) \\ & + \sum_{i=1}^q \sum_{i < j} \theta_i \theta_j \chi_1^\top(t) [\rho_j (\Xi_{1ij} + \#(\mathfrak{X}_1 \Delta \mathfrak{A} \mathcal{J}_2^1 - \Lambda_{1i}) \\ & + \rho_i (\Xi_{1ji} + \#(\mathfrak{X}_1 \Delta \mathfrak{A} \mathcal{J}_2^1 - \Lambda_{1j}) + \Lambda_{1i} + \Lambda_{1j}) \chi_1(t). \end{aligned} \quad (33)$$

In terms of (16)–(18) with $l = 1$, the right-hand side of (33) is ensured to be negative, which implies $\mathcal{J}(t) < 0$.

Case II ($t \in \mathcal{T}_2$): The system (13) is formed as

$$\begin{aligned} \dot{x}(t) = & \sum_{j=1}^q \theta_j \vartheta_j^k [(\mathfrak{A}_i + \Delta \mathfrak{A})x(t) \\ & + \mathfrak{B} \mathfrak{K}_j (\mathfrak{C} \mathcal{S} \mathbb{W}_x(t) - e(t)) + \mathfrak{F} \varpi(t)]. \end{aligned} \quad (34)$$

Based on the form in (34), one has

$$\sum_{i=1}^q \sum_{j=1}^q \theta_i \vartheta_j^k \mathfrak{G}_{2ij} \chi_2(t) = 0 \quad (35)$$

with $\chi_2^\top(t) \triangleq [\hat{x}^\top(t) \ x^\top(t) \ x^\top(t - \eta) \ x^\top(t - \lambda) \ \mathbb{W}_x^\top(t) \ e^\top(t) \ \varpi^\top(t) \ z^\top(t)]$.

In terms of (27), it gives

$$\xi(t) = \mathfrak{M}_2 \chi_2(t), \quad \dot{\xi}(t) = \mathfrak{N}_2 \chi_2(t). \quad (36)$$

With the aid of Jensen inequality and $\mathfrak{R}_5 > 0$, $-\eta_e \int_{-\eta}^0 b(\mathfrak{R}_5, x(t + s)) ds$ is relaxed as

$$-\eta_e \int_{-\eta}^0 b(\mathfrak{R}_5, x(t + s)) ds \leq -\frac{\eta_e}{\eta} b(\mathbb{I}_2^\top \mathfrak{R}_5 \mathbb{I}_2, \chi_2(t)). \quad (37)$$

According to $x^*(t) = \mathcal{S} \mathbb{W}_x(t) = \mathcal{J}_5^2 \chi_2(t)$, $e(t) = \mathcal{J}_{6+\kappa}^2 \chi_2(t)$, and the triggering rule (8), it results in

$$\begin{aligned} & b(\sigma_M \mathcal{S}^\top \mathfrak{C}^\top \Omega \mathfrak{C} \mathcal{S}, \mathcal{J}_5^2 \chi_2(t)) - b(\Omega, \mathcal{J}_{6+\kappa}^2 \chi_2(t)) \\ & \geq b(\sigma(t) \Omega, g^*(t)) - b(\Omega, e(t)) > 0. \end{aligned} \quad (38)$$

By integrating (24) and (36)–(38), it yields

$$\chi_2^\top(t) \mathbb{I}_2 \chi_2(t) < 0. \quad (39)$$

From (34) and the selection of $\mathfrak{X}_2 = X \mathcal{J}_2^1 + \mu X \mathcal{J}_2^2$, one gets

$$\sum_{i=1}^q \sum_{j=1}^q \theta_i \vartheta_j^k \chi_2^\top(t) \#(\mathfrak{X}_2 \mathfrak{G}_{2ij}) \chi_2(t) < 0. \quad (40)$$

Summing (39) and (40), we obtain

$$\sum_{i=1}^q \sum_{j=1}^q \theta_i \vartheta_j^k \chi_2^\top(t) (\Xi_{2ij} + \#(\mathfrak{X}_2 \Delta \mathfrak{A} \mathfrak{J}_2^2) \chi_2(t) < 0 \quad (41)$$

where $\Xi_{2ij} = \Pi_2 + \#(\mathfrak{X}_2 \mathfrak{G}_{2ij})$.

By taking the same method in the abovementioned case, it leads to $\mathcal{J}(t) < 0$ for this case.

In terms of the abovementioned two cases, the following condition is achieved:

$$\mathcal{V}(t) \leq -z^\top(t)z(t) + \gamma^2 \varpi^\top(t)\varpi(t). \quad (42)$$

From (42), we derive

$$V(\infty) - V(0) \leq \int_0^\infty (\gamma^2 \varpi^\top(t)\varpi(t) - z^\top(t)z(t)) dt. \quad (43)$$

If $\varpi(t) = 0$, it is easy to obtain $\mathcal{V}(t) < 0$ from (23), which denotes the system (13) is exponentially stable with a decay rate ς . If $\varpi(t) \neq 0$ and $x(0) = 0$, it follows that $\int_0^\infty z^\top(t)z(t) dt \leq \gamma^2 \int_0^\infty \varpi^\top(t)\varpi(t) dt$ from (43). These finish the proof. ■

Remark 5: In [29], Legendre polynomials are utilized to approach the distributed delay kernel $w(s)$, which could lead to approximation error and design conservativeness. In contrast to this treatment, a less conservative Lemma 1 proposed in [28] is applied to deal with the distributed delay term, which removes the approximation error. Moreover, Lemma 1 includes the integral inequality in [29] as a particular case by choosing $w(s)$ as Legendre polynomials.

Here, we are in place to solve the event-triggered controller design conditions given in Theorem 2.

Theorem 2: For given positive scalars ρ_j , σ_M , η , λ , μ , and ν , the uncertain T-S fuzzy system (13) under the adaptive weighted WMETM (8) is exponentially stable, satisfying the decay rate ς and H_∞ level γ , if there exist symmetric matrices $\hat{\mathfrak{R}}_1, \hat{\mathfrak{R}}_i > 0$ ($i = 2, 3, 4, 5$), $\hat{\mathfrak{R}}_5 > 0$, and matrices $\hat{\Lambda}_{li}$, \mathfrak{L}_j , and M such that

$$\hat{\mathfrak{R}}_1 > 0 \quad (44)$$

$$\begin{bmatrix} \rho_j (\hat{\Xi}_{lij} - \hat{\Lambda}_{li}) & * & * \\ \nu (\hat{\mathfrak{X}}_l^\top \mathfrak{D}_1)^\top & -\nu I & * \\ \mathfrak{D}_2 M \mathfrak{J}_2^l & 0 & -\nu I \end{bmatrix} < 0 \quad (45)$$

$$\begin{bmatrix} \rho_i (\hat{\Xi}_{lii} - \hat{\Lambda}_{li}) + \hat{\Lambda}_{li} & * & * \\ \nu (\hat{\mathfrak{X}}_l^\top \mathfrak{D}_1)^\top & -\nu I & * \\ \mathfrak{D}_2 M \mathfrak{J}_2^l & 0 & -\nu I \end{bmatrix} < 0 \quad (46)$$

$$\begin{bmatrix} \Theta_{lij} & * & * & * & * \\ \nu (\hat{\mathfrak{X}}_l^\top \mathfrak{D}_1)^\top & -\nu I & * & * & * \\ \mathfrak{D}_2 M \mathfrak{J}_2^l & 0 & -\nu I & * & * \\ \nu (\hat{\mathfrak{X}}_l^\top \mathfrak{D}_1)^\top & 0 & 0 & -\nu I & * \\ \mathfrak{D}_2 M \mathfrak{J}_2^l & 0 & 0 & 0 & -\nu I \end{bmatrix} < 0 \quad (47)$$

$$\begin{bmatrix} -\delta I & * \\ Y \mathfrak{C} - \mathfrak{C} M & -I \end{bmatrix} < 0 \quad (48)$$

for $l = 1, 2$, where

$$\Theta_{lij} = \rho_j (\hat{\Xi}_{lij} - \hat{\Lambda}_{li}) + \rho_i (\hat{\Xi}_{lii} - \hat{\Lambda}_{li}) + \hat{\Lambda}_{li} + \hat{\Lambda}_{lj}$$

$$\tilde{\mathfrak{R}}_1 = \hat{\mathfrak{R}}_1 + \text{diag}\{0, \lambda_e(\Psi \otimes \hat{\mathfrak{R}}_3)\}$$

$$\hat{\Xi}_{1ij} = \hat{\Pi}_1 + \#(\hat{\mathfrak{X}}_1 \hat{\mathfrak{G}}_{1ij})$$

$$\hat{\Pi}_1 = \#(\mathfrak{M}_1^\top \hat{\mathfrak{R}}_1 \mathfrak{M}_1) + 2\varsigma \mathfrak{b}(\hat{\mathfrak{R}}_1, \mathfrak{M}_1)$$

$$+ \#(\mathfrak{J}_{8+\kappa}^1 \mathfrak{C} M \mathfrak{J}_2^1) - \frac{\eta_e}{\eta} \mathfrak{b}(\hat{\mathfrak{R}}_5, \mathbb{I}_1) + \hat{F}^1$$

$$\hat{\mathfrak{X}}_1 = (\mathfrak{J}_1^1 + \mu \mathfrak{J}_2^1)^\top, \quad \hat{\mathfrak{R}}_5 = \begin{bmatrix} \hat{\mathfrak{R}}_5 & \hat{U} \\ \hat{U}^\top & \hat{\mathfrak{R}}_5 \end{bmatrix}$$

$$\hat{\mathfrak{G}}_{1ij} = \mathfrak{A}_i M \mathfrak{J}_2^1 + \mathfrak{B} \mathfrak{L}_j \mathfrak{C} \mathfrak{J}_{6+\kappa}^1 + \mathfrak{F} \mathfrak{J}_{7+\kappa}^1 - M \mathfrak{J}_1^1$$

$$\hat{F}^1 = \text{diag}\{\hat{F}_1^1, \hat{F}_2^1, \hat{F}_3^1, \hat{F}_4^1, \hat{F}_5^1, 0_8, F_7^1, -I\}$$

$$\hat{F}_1^1 = \eta \hat{\mathfrak{R}}_5, \quad \hat{F}_2^1 = \hat{\mathfrak{R}}_2, \quad \hat{F}_3^1 = \hat{\mathfrak{R}}_3 + \lambda \hat{\mathfrak{R}}_4 - \eta_e \hat{\mathfrak{R}}_2$$

$$\hat{F}_4^1 = -\lambda_e \hat{\mathfrak{R}}_3, \quad \hat{F}_5^1 = -\lambda_e(\Psi \otimes \hat{\mathfrak{R}}_4)$$

$$\hat{\Xi}_{2ij} = \hat{\Pi}_2 + \#(\hat{\mathfrak{X}}_2 \hat{\mathfrak{G}}_{2ij}), \quad \hat{\mathfrak{X}}_2 = (\mathfrak{J}_1^2 + \mu \mathfrak{J}_2^2)^\top$$

$$\hat{\Pi}_2 = \#(\mathfrak{M}_2^\top \hat{\mathfrak{R}}_1 \mathfrak{M}_2) + 2\varsigma \mathfrak{M}_2^\top \hat{\mathfrak{R}}_1 \mathfrak{M}_2$$

$$+ \#(\mathfrak{J}_{8+\kappa}^2 \mathfrak{C} M \mathfrak{J}_2^2) - \frac{\eta_e}{\eta} \mathfrak{b}(\hat{\mathfrak{R}}_5, \mathbb{I}_2) + \hat{F}^2$$

$$\hat{\mathfrak{G}}_{2ij} = \mathfrak{A}_i M \mathfrak{J}_2^2 + \mathfrak{B} \mathfrak{L}_j \mathfrak{C} \mathfrak{J}_5^2 - \mathfrak{B} \mathfrak{L}_j \mathfrak{J}_{6+\kappa}^2 + \mathfrak{F} \mathfrak{J}_{7+\kappa}^2 - M \mathfrak{J}_1^2$$

$$\hat{F}^2 = \text{diag}\{\hat{F}_1^2, \hat{F}_2^2, \hat{F}_3^2, \hat{F}_4^2, \hat{F}_5^2, \hat{F}_6^2, F_7^2, -I\}$$

$$\hat{F}_1^2 = \hat{F}_1^1, \quad \hat{F}_2^2 = \hat{F}_2^1, \quad \hat{F}_3^2 = \hat{F}_3^1, \quad \hat{F}_4^2 = \hat{F}_4^1$$

$$\hat{F}_5^2 = -\lambda_e(\Psi \otimes \hat{\mathfrak{R}}_4) + \sigma_M \mathfrak{b}(\hat{\Omega}, \mathfrak{C} \mathfrak{J}), \quad \hat{F}_6^2 = -\hat{\Omega}.$$

Then, the fuzzy controller parameters are derived by $\mathfrak{K}_j = \mathfrak{L}_j Y^{-1}$.

Proof: Define $M = X^{-1}$, $\hat{\mathfrak{R}}_i = M \mathfrak{R}_i M$ ($i = 2, \dots, 5$), $\hat{\Omega} = Y \Omega Y$, $\hat{\mathfrak{R}}_1 = (I_{\kappa+1} \otimes M) \mathfrak{R}_1 (I_{\kappa+1} \otimes M)$, $Y \mathfrak{C} = \mathfrak{C} M$, and $\mathfrak{L}_j \mathfrak{C} = \mathfrak{K}_j \mathfrak{C} M$.

Applying (5) to (16) with $l = 1$, we have

$$\rho_j (\Xi_{1ij} - \Lambda_{1i}) + \nu \mathfrak{X}_1^\top \mathfrak{D}_1 (\mathfrak{X}_1^\top \mathfrak{D}_1)^\top + \nu^{-1} (\mathfrak{D}_2 \mathfrak{J}_2^1)^\top \mathfrak{D}_2 \mathfrak{J}_2^1 < 0. \quad (49)$$

According to the Schur complement, one can obtain

$$\begin{bmatrix} \rho_j (\Xi_{1ij} - \Lambda_{1i}) & * & * \\ \nu (\mathfrak{X}_1^\top \mathfrak{D}_1)^\top & -\nu I & * \\ \mathfrak{D}_2 \mathfrak{J}_2^1 & 0 & -\nu I \end{bmatrix} < 0. \quad (50)$$

Multiplying both left- and right-hands of (16) by $\mathbb{M}_1^\top = \text{diag}\{M, M, M, M, I_{\kappa+1} \otimes M, M, I, I, I, I, I\}^\top$ and \mathbb{M}_1 , one has

$$\begin{bmatrix} \rho_j (\hat{\Xi}_{1ij} - \hat{\Lambda}_{1i}) & * & * \\ \nu (\hat{\mathfrak{X}}_1^\top \mathfrak{D}_1)^\top & -\nu I & * \\ \mathfrak{D}_2 M \mathfrak{J}_2^1 & 0 & -\nu I \end{bmatrix} < 0 \quad (51)$$

where $\hat{\Lambda}_{1i} = \mathbb{M}_{11}^\top \Lambda_{1i} \mathbb{M}_{11}$.

Following the similar way and choosing $\mathbb{M}_2^\top = \text{diag}\{M, M, M, M, I_{\kappa+1} \otimes M, Y, I, I, I, I, I\}^\top$, (46) and (47)

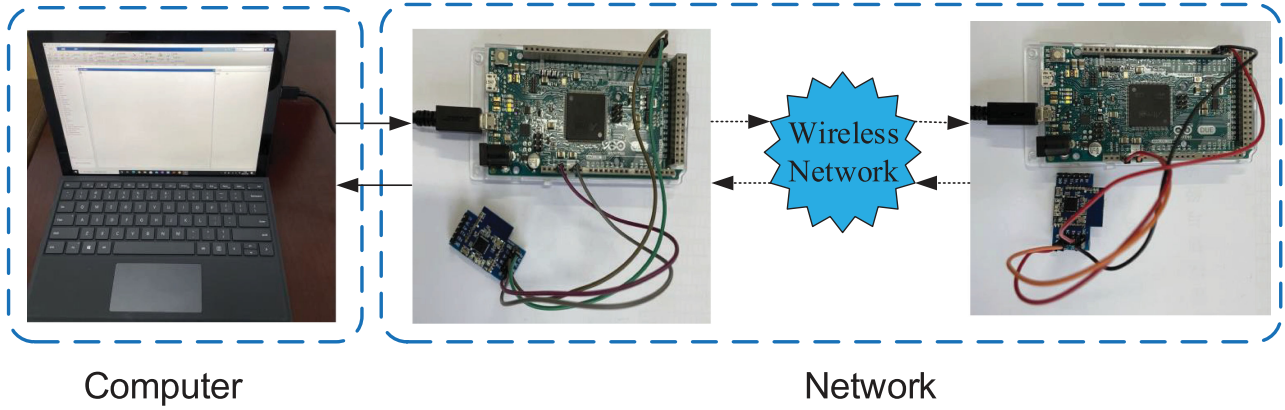


Fig. 2. Experiment setup.

can be achieved. By choosing $\mathbb{M}_3^\top = \text{diag}\{M, I_{\kappa+1} \otimes M\}^\top$, (44) is derived.

It is noted that $Y\mathcal{C} = \mathcal{C}M$ has no feasible solution, because it is not a strict inequality. Then, the issue of dealing with the nonlinear term $X^\top \mathfrak{B} \mathfrak{R}_j \mathcal{C}$ in Theorem 1 can be treated as a W -problem [32].

Based on $Y\mathcal{C} = \mathcal{C}M$, we obtain

$$(Y\mathcal{C} - \mathcal{C}M)^\top (Y\mathcal{C} - \mathcal{C}M) = 0. \quad (52)$$

Adopting Schur complement to (52), it is further transformed as the following optimization problem:

$$\begin{bmatrix} -\delta I & * \\ Y\mathcal{C} - \mathcal{C}M & -I \end{bmatrix} < 0 \quad (53)$$

which is equivalent to the condition (48) with a sufficient small scalar $\delta > 0$.

Therefore, the proof is completed. \blacksquare

Remark 6: The derived conditions in Theorem 2 are solved by LMI toolbox in MATLAB. The computation complexity of solving these conditions mainly relies on the size of Lyapunov matrix \mathfrak{R}_1 , which is related to the degree κ of the vector $w(s)$. That is to say, the computation complexity is growing as the increase of κ .

IV. EXAMPLE

In this section, we build up an experimental setup integrating computer and real wireless network to execute the developed event-triggered control strategy. It is shown in Fig. 2 that the uncertain fuzzy WTS, the adaptive METM, and the controller are implemented in MATLAB/Simulink software in computer. And the event-triggered control signals are transmitted over a practical wireless network composed by Zigbee devices. The sampling period of the Zigbee devices is 0.001 s. In this example, 2 bytes are used to represent one control signal. Since two measured signals $g_1(t_k)$ and $g_2(t_k)$ are transmitted, the length of one data packet is 11 bytes according to the packet formation table given in [25]. It is seen from Fig. 2 that the ZigBee modules connected with the computer is utilized to transmit and receive the triggered signals over the network. And each data packet will

TABLE I
WTS PARAMETERS

\mathbb{J}	$5 \times 10^{-3} N \cdot m$	\mathbb{R}	$0.5 m$
ϑ	$1.2 kg/m^2$	\mathbb{Q}_f	$0.16 Wb$
ρ	$6 \times 10^{-3} N \cdot m \cdot s/rad$	\mathbb{R}	$5 \times 10^{-3} N \cdot m$
$\mathbb{L}_d = \mathbb{L}_q$	$2.7 \times 10^{-3} H$	\mathbb{R}_s	1.13Ω
\mathbb{P}_n	8	$\mathbb{C}_{P \max}$	0.41
$\alpha_{opt}(t)$	8.1	$\mathbb{D}_1 = -\mathbb{D}_2$	5

be transmitted twice, that is, from the left ZigBee to the right ZigBee, and from the right one to the left one.

We choose the same parameters of PMSG-based WTS [8], which are given in Table I.

The weighting function $w(s)$, $s \in [-\eta, 0]$ is taken as

$$w(s) = \frac{\pi}{2\eta} \cos\left(\frac{\pi}{2\eta} s\right)$$

$$w(s) = \begin{bmatrix} \frac{\pi}{2\eta} \cos\left(\frac{\pi}{2\eta} s\right) \\ \frac{\pi}{2\eta} \sin\left(\frac{\pi}{2\eta} s\right) \end{bmatrix}, \mathcal{W} = \begin{bmatrix} 0 & -\frac{\pi}{2\eta} \\ \frac{\pi}{2\eta} & 0 \end{bmatrix}.$$

Consider the other parameters as $\delta = 0.01$, $\sigma = 0.2$, $\lambda = 0.006$, $\eta = 0.002$, $\mu = 1500$, $\nu = 0.01$, $\varsigma = 0.01$, $\Delta R = 0.5 \sin(t)$, and $d = 0.5$. Thus, the membership functions of the fuzzy controller (10) meeting $\vartheta_j^k - \rho_j \theta_j \geq 0$ are chosen the same in [8] as $\vartheta_1(x_1(t)) = 0.5e^{-x_1^2(t)/5.5}$ and $\vartheta_2(x_1(t)) = 1 - \vartheta_1(x_1(t))$ with $\rho_1 = \rho_2 = 0.9$. By solving the controller design conditions in Theorem 2, it gives

$$\mathfrak{R}_1 = \begin{bmatrix} 0.0413 & -0.0242 \\ -0.0014 & -0.0045 \end{bmatrix}, \mathfrak{R}_2 = \begin{bmatrix} 0.0425 & -0.0238 \\ -0.0004 & 0.0046 \end{bmatrix}$$

$$\Omega = \begin{bmatrix} 10.4973 & 1.7224 \\ 1.7224 & 8.0432 \end{bmatrix}.$$

The initial condition is taken as $x(0) = [5 \quad -2 \quad 3]^\top$ and the simulation period is 0.001 s. Considering the stochastic changes of changes of operation conditions, the external disturbance is

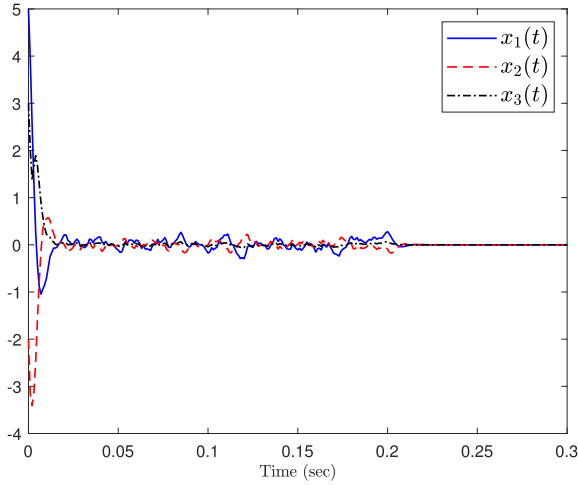
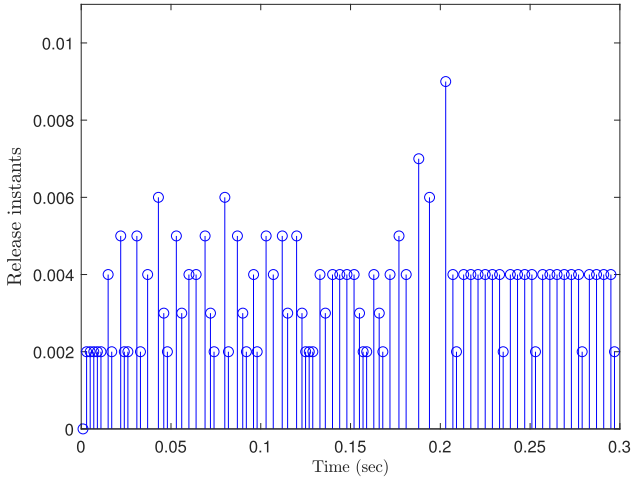
Fig. 3. Responses of system state $x(t)$.

Fig. 4. Release instants and time intervals.

chosen as $\varpi(t) = \mathbb{U}_f(t)$ for $0 < t < 0.2$ s (otherwise, $\varpi(t) = 0$), where $\mathbb{U}_f(t)$ is a stochastic variable satisfying the uniform distribution and $|\mathbb{U}_f(t)| \leq 10$. By utilizing the controller gains and the parameters of METM in (8), the state responses of the uncertain WTS are shown in Fig. 3. Fig. 4 shows the sequence of event-triggering instants. From Figs. 3 and 4, it can be seen that the system under the memory-event-triggered controller operates in stability by updating the control signal 84 times. Moreover, to show the interconnection between the threshold $\sigma(t)$ and the triggering frequency over the interval $[t_1, t_2]$, we introduce

$$\bar{\sigma} \triangleq \frac{\int_{t_1}^{t_2} \sigma(t) dt}{t_2 - t_1}, \quad \bar{h} \triangleq \frac{t_2 - t_1}{\mathcal{N}}$$

as the average threshold ($\bar{\sigma}$) and the average triggering period (\bar{h}), respectively, where \mathcal{N} represents the number of triggers. Thus, one also observes that the average threshold and the average triggering period over $\mathbb{T}_1 \triangleq [0, 0.2]$ s are $\bar{\sigma} = 0.1699$, $\bar{h} = 0.0031$ s, and the corresponding values over $\mathbb{T}_2 \triangleq [0.2, 0.3]$ s are $\bar{\sigma} = 0.286$ and $\bar{h} = 0.0036$ s. It means that in \mathbb{T}_1 , a smaller triggering threshold $\sigma(t)$ is executed to generate more control

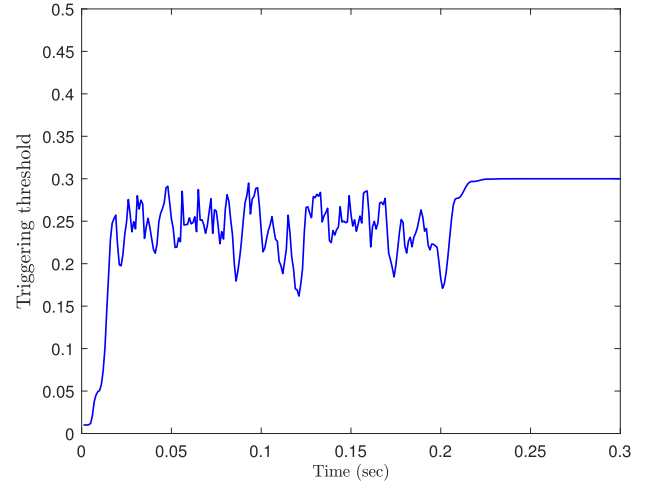
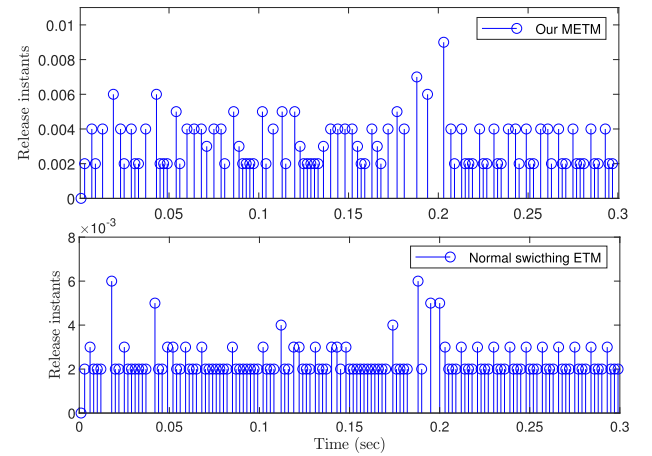
Fig. 5. Triggering threshold $\sigma(t)$.

Fig. 6. Release instants and time intervals under our METM and normal switching ETM.

signals to stabilize the system, and then $\sigma(t)$ is increased to reduce data transmission when the system converges to be stable.

In addition, the following comparison results are executed to illustrate the advantage of the proposed METM (8) over the switching ETM in [15]. For a fair comparison, a constant triggering threshold $\sigma(t) = \sigma_m = \sigma_M = 0.2$ is taken.

By solving Theorem 2 with the same parameters in abovementioned calculation, the controller gains and triggering matrix are obtained as

$$\mathfrak{K}_1 = \begin{bmatrix} 0.0354 & -0.0208 \\ -0.0020 & -0.0047 \end{bmatrix}, \quad \mathfrak{K}_2 = \begin{bmatrix} 0.0371 & -0.0198 \\ 0.0004 & 0.0044 \end{bmatrix}$$

$$\Omega = \begin{bmatrix} 11.6673 & 1.8266 \\ 1.8266 & 8.8862 \end{bmatrix}.$$

The initial condition $x(0) = [1 \ 0.5 \ -1]^\top$ and the same external disturbance are considered. The triggering time and intervals under two different ETMs are shown in Fig. 6. The number of released events are given in Table II.

TABLE II
NUMBER OF TRIGGERED EVENTS \mathcal{N}

Method	\mathcal{N}
Our METM (8)	94
Normal switching ETM in [15]	126

In terms of Fig. 6 and Table II, it is observed that our proposed METM has decreased the triggered events by 25.4% compared with the normal ETM. This indicates the better ability of suppressing the unnecessary triggers caused by random data jitters under the METM with historic outputs than the existing switching ETM only using instantaneous system information.

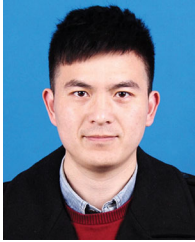
V. CONCLUSION

The problem of adaptive memory-event-triggered H_∞ static output control for uncertain T-S fuzzy WTSs has been investigated in this article. The weighted mean of historic outputs was used in the design of the METM to replace the present output, by which it was able to further reduce the unnecessary transmission and improve the robustness of the METM against dramatical disturbances and noises. Additionally, the adaptive triggering threshold was introduced to dynamically regulate the triggering frequency along with weighted mean of historic outputs. By selecting a novel LKF related with the weighting function, we presented some sufficient stability analysis and control synthesis conditions via a set of LMIs. A hardware-in-loop experimental platform composed of ZigBee modules was established to demonstrate the advantages of the provided approach. Since the communication delay and secure transmission are significant problems of network, the proposed adaptive METM will be applied to the stability analysis and stabilization for WTSs with time-varying delays and cyber-attacks.

REFERENCES

- [1] S. Lu, Y. Wu, S. Lou, and X. Yin, "A model for power system transmission network expansion planning under low-carbon economy," in *Proc. IEEE Power Energy Soc. Gen. Meeting*, 2013, pp. 1–5.
- [2] B. Cao, W. Dong, Z. Lv, Y. Gu, S. Singh, and P. Kumar, "Hybrid microgrid many-objective sizing optimization with fuzzy decision," *IEEE Trans. Fuzzy Syst.*, vol. 28, no. 11, pp. 2702–2710, Nov. 2020.
- [3] D. Pudjianto, M. Aunedi, P. Djapic, and G. Strbac, "Whole-systems assessment of the value of energy storage in low-carbon electricity systems," *IEEE Trans. Smart Grid*, vol. 5, no. 2, pp. 1098–1109, Mar. 2014.
- [4] Y. Li *et al.*, "Optimal stochastic operation of integrated low-carbon electric power, natural gas, and heat delivery system," *IEEE Trans. Sustain. Energy*, vol. 9, no. 1, pp. 273–283, Jan. 2018.
- [5] P. Mani, R. Rajan, L. Shanmugam, and Y. H. Joo, "Adaptive fractional fuzzy integral sliding mode control for PMSM model," *IEEE Trans. Fuzzy Syst.*, vol. 27, no. 8, pp. 1674–1686, Aug. 2019.
- [6] V. Gandhi and Y.-H. Joo, "T-S fuzzy sampled-data control for non-linear systems with actuator faults and its application to wind energy system," *IEEE Trans. Fuzzy Syst.*, early access, Nov. 27, 2020, doi: [10.1109/TFUZZ.2020.3041113](https://doi.org/10.1109/TFUZZ.2020.3041113).
- [7] A. Rajaei, M. Mohamadian, and A. Y. Varjani, "Vienna-rectifier-based direct torque control of PMSG for wind energy application," *IEEE Trans. Ind. Electron.*, vol. 60, no. 7, pp. 2919–2929, Jul. 2013.
- [8] S. Hwang, J. B. Park, and Y.-H. Joo, "Disturbance observer-based integral fuzzy sliding-mode control and its application to wind turbine system," *IET Control Theory Appl.*, vol. 13, no. 12, pp. 1891–1900, Jul. 2019.
- [9] B. Herissi and D. Boudjehem, "Fractional-order fuzzy controller for a PMSG wind turbine system," *Int. J. Syst. Sci.*, vol. 51, no. 16, pp. 3237–3250, Aug. 2020.
- [10] A. Vinodkumar, M. Prakash, and Y. H. Joo, "Impulsive observer-based output control for PMSG-based wind energy conversion system," *IET Control Theory Appl.*, vol. 13, no. 13, pp. 2056–2064, Jul. 2019.
- [11] E. Bijami and M. M. Farsangi, "Networked distributed automatic generation control of power system with dynamic participation of wind turbines through uncertain delayed communication network," *IET Renewable Power Gener.*, vol. 11, no. 8, pp. 1254–1269, Jun. 2017.
- [12] A. Ouammi, Y. Achour, D. Zejli, and H. Dagdougui, "Supervisory model predictive control for optimal energy management of networked smart greenhouses integrated microgrid," *IEEE Trans. Autom. Sci. Eng.*, vol. 17, no. 1, pp. 117–128, Jan. 2020.
- [13] A. R. Malekpour and A. Pahwa, "Stochastic networked microgrid energy management with correlated wind generators," *IEEE Trans. Power Syst.*, vol. 32, no. 5, pp. 3681–3693, Sep. 2017.
- [14] L. Wang, Z. Wang, Q.-L. Han, and G. Wei, "Event-based variance-constrained H_∞ filtering for stochastic parameter systems over sensor networks with successive missing measurements," *IEEE Trans. Cybern.*, vol. 48, no. 3, pp. 1007–1017, Mar. 2018.
- [15] A. Selivanov and E. Fridman, "Event-triggered H_∞ control: A switching approach," *IEEE Trans. Autom. Control*, vol. 61, no. 10, pp. 3221–3226, Oct. 2016.
- [16] S. Yan, M. Shen, S. K. Nguang, and G. Zhang, "Event-triggered H_∞ control of networked control systems with distributed transmission delay," *IEEE Trans. Autom. Control*, vol. 65, no. 10, pp. 4295–4301, Oct. 2020.
- [17] Z. Gu, X. Sun, H.-K. Lam, D. Yue, and X. Xie, "Event-based secure control of T-S fuzzy based 5-DOF active semi-vehicle suspension systems subject to DoS attacks," *IEEE Trans. Fuzzy Syst.*, early access, Apr. 14, 2021, doi: [10.1109/TFUZZ.2021.3073264](https://doi.org/10.1109/TFUZZ.2021.3073264).
- [18] L. Wang, Z. Wang, G. Wei, and F. E. Alsaadi, "Finite-time state estimation for recurrent delayed neural networks with component-based event-triggering protocol," *IEEE Trans. Neural Netw. Learn. Syst.*, vol. 29, no. 4, pp. 1046–1057, Apr. 2018.
- [19] Z. Feng, Y. Yang, and H.-K. Lam, "Extended-dissipativity-based adaptive event-triggered control for stochastic polynomial fuzzy singular systems," *IEEE Trans. Fuzzy Syst.*, early access, Aug. 25, 2021, doi: [10.1109/TFUZZ.2021.3107753](https://doi.org/10.1109/TFUZZ.2021.3107753).
- [20] S. Yan, S. K. Nguang, and Z. Gu, " H_∞ weighted integral event-triggered synchronization of neural networks with mixed delays," *IEEE Trans. Ind. Inform.*, vol. 17, no. 4, pp. 2365–2375, Apr. 2021.
- [21] Z. Gu, T. Yin, and Z. Ding, "Path tracking control of autonomous vehicles subject to deception attacks via a learning-based event-triggered mechanism," *IEEE Trans. Neural Netw. Learn. Syst.*, vol. 32, no. 12, pp. 5644–5653, Dec. 2021, doi: [10.1109/TNNLS.2021.3056764](https://doi.org/10.1109/TNNLS.2021.3056764).
- [22] M. Prakash and Y.-H. Joo, "Fuzzy event-triggered control for back to back converter involved PMSG-based wind turbine systems," *IEEE Trans. Fuzzy Syst.*, early access, Feb. 17, 2021, doi: [10.1109/TFUZZ.2021.3059949](https://doi.org/10.1109/TFUZZ.2021.3059949).
- [23] G. Nagamani, Y. H. Joo, G. Soundararajan, and R. Mohajerpour, "Robust event-triggered reliable control for T-S fuzzy uncertain systems via weighted based inequality," *Inf. Sci.*, vol. 512, pp. 31–49, Feb. 2020.
- [24] S. H. Mousavi and H. J. Marquez, "Integral-based event triggering controller design for stochastic LTI systems via convex optimisation," *Int. J. Control*, vol. 89, no. 7, pp. 1416–1427, Jan. 2016.
- [25] S. Yan, M. Shen, S. K. Nguang, G. Zhang, and L. Zhang, "A distributed delay method for event-triggered control of T-S fuzzy networked systems with transmission delay," *IEEE Trans. Fuzzy Syst.*, vol. 27, no. 10, pp. 1963–1973, Oct. 2019.
- [26] M. Rosyadi, S. M. Mueen, R. Takahashi, and J. Tamura, "Stabilization of fixed speed wind generator by using variable speed PM wind generator in multi-machine power system," in *Proc. 15th Int. Conf. Elect. Mach. Syst.*, 2012, pp. 1–6.
- [27] T. Ackermann, *Wind Power in Power Systems*. Hoboken, NJ, USA: Wiley, 2005.
- [28] Q. Feng and S. K. Nguang, "Stabilization of uncertain linear distributed delay systems with dissipativity constraints," *Syst. Control Lett.*, vol. 96, pp. 60–71, Oct. 2016.
- [29] A. Seuret, F. Gouaisbaut, and Y. Ariba, "Complete quadratic Lyapunov functionals for distributed delay systems," *Automatica*, vol. 62, pp. 168–176, Dec. 2015.
- [30] P. Park, J. W. Ko, and C. Jeong, "Reciprocally convex approach to stability of systems with time-varying delays," *Automatica*, vol. 47, no. 1, pp. 235–238, Jan. 2011.

- [31] Y. Wang, L. Xie, and C. E. De Souza, "Robust control of a class of uncertain nonlinear systems," *Syst. Control Lett.*, vol. 19, no. 2, pp. 139–149, Aug. 1992.
- [32] C. A. Crusius and A. Trofino, "Sufficient LMI conditions for output feedback control problems," *IEEE Trans. Autom. Control*, vol. 44, no. 5, pp. 1053–1057, May 1999.



Shen Yan received the B.E. degree in automation and Ph.D. degree in power engineering automation from the College of Electrical Engineering and Control Science of Nanjing Technology University, Nanjing, China, in 2014 and 2019, respectively.

From 2017 to 2018, he was a Visiting Ph.D. Student with the University of Auckland, Auckland, New Zealand. He is currently a Lecturer with the College of Mechanical and Electronic Engineering, Nanjing Forestry University, Nanjing, China. His research interests include networked control systems and event-triggered control and their applications.

triggered control and their applications.



Zhou Gu (Member, IEEE) received the B.S. degree in automation from North China Electric Power University, Beijing, China, in 1997, and the M.S. and Ph.D. degrees in control science and engineering from the Nanjing University of Aeronautics and Astronautics, Nanjing, China, in 2007 and 2010, respectively.

From 1996 to 2013, he was an Associate Professor with the School of Power engineering, Nanjing Normal University, Nanjing. He was a Visiting Scholar with Central Queensland University, Rockhampton, QLD, Australia, and The University of Manchester,

Manchester, U.K. He is currently a Professor with Nanjing Forestry University, Nanjing. His research interests include networked control systems, time-delay systems, and reliable control and their applications.



Ju H. Park (Senior Member, IEEE) received the Ph.D. degree in electronics and electrical engineering from the Pohang University of Science and Technology (POSTECH), Pohang, Korea, in 1997.

From May 1997 to February 2000, he was a Research Associate with Engineering Research Center-Automation Research Center, POSTECH. In March 2000, he joined Yeungnam University, Kyongsan, Korea, where he is currently the Chuma Chair Professor. He is a co-author of the monographs *Recent Advances in Control and Filtering of Dynamic Systems with Constrained Signals* (Springer-Nature, 2018) and *Dynamic Systems With Time Delays: Stability and Control* (Springer-Nature, 2019), and is an Editor of an edited volume *Recent Advances in Control Problems of Dynamical Systems and Networks* (Springer-Nature, 2020). He has authored or coauthored a number of articles in the areas of his research interest, which include robust control and filtering, neural/complex networks, fuzzy systems, multiagent systems, and chaotic systems.

Prof. Park is a Fellow of the Korean Academy of Science and Technology. In 2015, he was the recipient of the Highly Cited Researchers Award by Clarivate Analytics (formerly, Thomson Reuters) and was listed in three fields, engineering, computer sciences, and mathematics, in 2019, 2020, and 2021. He is an Editor of the *International Journal of Control, Automation and Systems*. He is also a Subject Editor, Advisory Editor, Associate Editor, and an Editorial Board Member of several international journals, including the *IET Control Theory & Applications*, *Applied Mathematics and Computation*, *Journal of The Franklin Institute*, *Nonlinear Dynamics*, *Engineering Reports*, *Cogent Engineering*, IEEE TRANSACTION ON FUZZY SYSTEMS, IEEE TRANSACTION ON NEURAL NETWORKS AND LEARNING SYSTEMS, and IEEE TRANSACTION ON CYBERNETICS.



Xiangpeng Xie received the B.S. and Ph.D. degrees in engineering from Northeastern University, Shenyang, China, in 2004 and 2010, respectively.

From 2010 to 2014, he was a Senior Engineer with the Metallurgical Corporation of China Ltd., Beijing, China. He is currently a Professor with the Institute of Advanced Technology, Nanjing University of Posts and Telecommunications, Nanjing, China. His research interests include fuzzy modeling and control synthesis, state estimations, optimization in process industries, and intelligent optimization algorithms.

Prof. Xie is an Associate Editor for the *International Journal of Control, Automation, and Systems*, and the *International Journal of Fuzzy Systems*.